Recovering Observability via Active Sensing

Abhinav Kunapareddy and Noah J. Cowan

Abstract— **Observability is a formal property of a system that ensures the ability to estimate the system's states from output measurements and knowledge of the inputs. In engineering, sensors are typically designed and deployed to guarantee observability irrespective of the control input, thereby simplifying control systems design. Here, we consider a class of nonlinear sensors that require 'persistently exciting' control inputs to maintain observability. This choice of sensor models is motivated by biological sensing systems which 'adapt' to constant stimuli, giving them a very high dynamic range, but leading to a phenomenon known as perceptual fading. To prevent perceptual fading, animals employ *active sensing* in the form of time-varying motor commands that continually stimulate sensory receptors. To capture this phenomenon, we introduce a simplified sensor model that requires active sensing inputs to maintain observability. Under certain assumptions, the input–output characteristics of the active sensing system is shown to be equivalent to an observable linear time-invariant (LTI) system. Using the framework of Harmonic Transfer Functions, the equivalent system is identified by (1) modulating the system via a sinusoidal active input, (2) demodulating the resulting output, and (3) low-pass filtering. This relatively simple framework for active sensing may pave the way for the design and deployment of adaptive sensory systems for engineering applications.**

I. Introduction

The dominant paradigm in feedback control theory is to decouple the problems of control and state estimation. This is called the separation principle. For example, for a linear plant corrupted with Gaussian noise a Kalman filter can be used for optimal state estimation, which can then be used to drive a linear-quadratic regulator (LQR). The separation principle allows us to design the Kalman filter and controller independently of one another; i.e., the Kalman filter does not depend on the LQR cost function, and the LQR gains do not depend on the sensory and process noise covariances.

However, for a general nonlinear plant, the separation principle does not hold. So, in order to facilitate the design of independent observers and controllers it may—or may not—be a good idea to start with linearization. For example, for a simple static nonlinearity in the vector field or output map, it may be a good idea to linearize the system around its equilibrium. However, certain categories of nonlinearities may preclude linear separability even if the system is both (nonlinearly) controllable and observable.

Indeed, we suspect that this paradigm (linearization as the first step in control design) does not apply to many biological control systems in animals. Biological sensory systems often stop responding to persistent (i.e. "DC") stimuli, a process known as "adaptation" in the neuroscience literature. Sensory adaptation makes asymptotically exact set-point control impossible due to the imperceptibility of large, slow drifts in the signal of interest. Animals often use a strategy known as active sensing [1]–[3] in which the organism generates potentially costly movements that do not necessarily directly serve a motor goal but improve sensory feedback and prevent perceptual fading [4]. Indeed, any searching behavior is a form of active sensing and many species of animals perform such behaviors. This paper focuses on developing a framework to use such active sensing movements to recover the observability for a simple biologically inspired nonlinear system. Since this is fundamentally a sensing / observability problem, we focus on linear plant dynamics with a *nonlinear output*, resulting in an overall nonlinear system.

Dept. of Mechanical Engineering, Johns Hopkins University, Baltimore, MD, USA akunapa1@jhu.edu, ncowan@jhu.edu

II. Active Sensing

A. Active Sensing in Biology and Engineering

Active sensing can be broadly defined as a feedback controlled system that expends energy to sense its surroundings [1], [2]. Active sensing is most commonly associated with species that generate and emit sensing signals, such as echolocation in bats [5], [6] or active electroreception in certain species of fish [7]. However, a more general form of active sensing involves energy expenditure via the system's own active movements [8]–[17]. Some examples of movement-based active sensing are movements of weakly electric fish [3], [18]–[21], active sensing in vision [22]–[24], whisking [25]–[29], active touch [30]–[33], sniffing [34]–[36] and hydrodynamic imaging [37]–[39].

During such movement-based active sensing, the animal's motor behavior does not linearly relate to its task-level goal and is often routinely changed in relation to the sensory demands [40]–[46]. This suggests that the animal's movement might be stimulating/altering the sensory signals it is receiving in order to better excite its sensors and downstream neural circuits, thereby improve task-level performance [3].

The fundamental goal of our work is to examine how active movements of a system, even if not directly related to the task, can nevertheless be used to improve the task-level performance in achieving a motor goal. Similar ideas have been explored in previous engineering work [47]–[52]. For the nonholonomic planar unicycle, for example, a periodically exciting control system renders the system nonlinearly observable, making it possible to design an observer-based feedback control system despite the existence of a "statically unobservable" submanifold [48]. Previous work on differentially flat systems involves optimizing control inputs to maximize observability [49]. For multi-robot systems, Mariottini et al. [50] designed a switching active control strategy to maintain formation control even when

all robots tend to move along non-observable paths, and for UAVs, Lalish et al. [51] used oscillatory inputs to control a system which is not small time locally controllable. Lastly, Hinson et al. [52] showed that, for first-order nonholonomic systems, active control actuation over at least two channels is required to maintain observability.

B. The "Simplest" System Requiring Active Sensing

In this section we introduce a simple (perhaps the simplest) biologically inspired sensory system that, when coupled with a mechanical system, requires active sensing to ensure observability. This model is motivated by ongoing studies of sensorimotor control in weakly electric knifefish in the LIMBS Laboratory in a simple one-degree-of-freedom refuge tracking behavior [3], [53]–[56].

Suppose x_1 is the position of the system and $x_2 = \dot{x}_1$ is its velocity as it moves in one degree of freedom according to the simple dynamics $m\dot{x}_2 + bx_2 = u$ as described for weakly electric fish [54]. To formalize the notion of sensory adaptation, we assume a receptor measures only the local rate of change of a stimulus as the system moves relative to a sensory scene $s(x_1)$, i.e., $y = \frac{d}{dt}s(x_1)$. Defining $g(x_1) = s'(x_1)$, we arrive at the following model, which is nonlinear due to the output y:

$$\begin{aligned} \dot{x} &= \underbrace{\begin{bmatrix} 0 & 1 \\ 0 & -\frac{b}{m} \end{bmatrix}}_{\text{A}} x + \underbrace{\begin{bmatrix} 0 \\ \frac{1}{m} \end{bmatrix}}_{\text{B}} u, \\ y &= g(x_1)x_2, \end{aligned} \tag{1}$$

where m is the mass, b is the damping and the control input u is the total external force acting on the system.

The linearization of (1) around any equilibrium, $(x_1^*, 0)$, is given by (A, B, C), where

$$C = \begin{bmatrix} 0 & g(x_1^*) \end{bmatrix} \tag{2}$$

Clearly, (A, C) is not observable irrespective of $g(x)$. The observability matrix of the system always loses rank due to output being proportional to the velocity of the sensor, making it impossible to infer its position (since the system is translationally invariant).

However, a simple rank condition test on the Lie derivatives of the system [57] shows that nonlinear observability is guaranteed for nonzero velocities, $x_2 \neq 0$:

$$\begin{aligned} \dot{x} &= Ax + Bu, \\ y &= g(x_1)x_2. \end{aligned}$$

Note that, this is not a Gramian test for linear systems, but rather a Jacobian rank condition test for nonlinear systems since the output nonlinearity precludes a linear test.

The Lie derivatives of the system are given by

$$\begin{aligned} h &= g(x_1)x_2, \\ L_f h &= g'(x_1)x_2^2 - g(x_1)x_2\frac{b}{m}. \end{aligned}$$

Following [57], we define the matrix G via

$$\begin{aligned} G &= \begin{bmatrix} h \\ L_f h \end{bmatrix} = \begin{bmatrix} g(x_1)x_2 \\ g'(x_1)x_2^2 - g(x_1)x_2\frac{b}{m} \end{bmatrix} \\ dG &= \begin{bmatrix} g'(x_1)x_2 & g(x_1) \\ g''(x_1)x_2^2 - g'(x_1)x_2\frac{b}{m} & 2g'(x_1)x_2 - g(x_1)\frac{b}{m} \end{bmatrix}. \end{aligned}$$

For the system to be nonlinearly observable we require that dG be full rank, which is guaranteed for nonzero determinant:

$$x_2^2(2(g'(x_1))^2 - g(x_1)g''(x_1)) \neq 0. \tag{3}$$

This simple result illustrates that control to a fixed position ($x_2 = 0$) results in a loss of not just linear observability, but also of *nonlinear observability*—i.e. it is a fundamental system property and not an artifact of linearization. And thus, to maintain observability, one must design a control input that sufficiently excites the sensory system to enable estimation of the states necessary for control.

C. Our System with Active Sensing

In this section, we try to excite the sensory system ("pumping" the system) with a time-periodic control signal $u^*(t)$. Specifically, we linearize the system (1) around a time varying equilibrium $(x^*(t), u^*(t))$ which results in the following approximate linear time-varying (LTV) system around the equilibrium $(x^*(t), u^*(t))$:

$$\begin{aligned} \delta\dot{x} &= A\delta x + B\delta u, \\ \delta y &= \left[\tfrac{\partial}{\partial x_1}g(x_1)x_2 \quad \tfrac{\partial}{\partial x_2}g(x_1)x_2\right]_{x=x^*}\delta x, \\ &= \begin{bmatrix} g'(x_1^*)x_2^* & g(x_1^*) \end{bmatrix}\delta x. \end{aligned}$$

Choosing $x_1^* = a\cos(\omega t)$ results in the equilibrium state $(x^*(t), u^*(t))$ given by

$$\begin{aligned} x^*(t) &= \begin{bmatrix} x_1^*(t) \\ \frac{d}{dt}x_1^*(t) \end{bmatrix} = \begin{bmatrix} a\cos(\omega t) \\ -a\omega\sin(\omega t) \end{bmatrix}, \\ u^*(t) &= -am\omega^2\cos(\omega t) - ab\omega\sin(\omega t), \end{aligned}$$

where m, b are the mass and damping of the system as specified in (1). To simplify notation, we will henceforth be representing δu as u and the total input to the system as $u_{\text{total}} = u + u^*$. Therefore the LTP system now is,

$$\begin{aligned} \delta\dot{x} &= A\delta x + Bu, \\ \delta y &= C(t)\delta x. \end{aligned} \tag{4}$$

where A, B are given by (2) and

$$C(t) = \begin{bmatrix} -g'\left(a\cos(\omega t)\right)a\omega\sin(\omega t) & g\left(a\cos(\omega t)\right) \end{bmatrix}.$$

This LTP system is now further analyzed and simplified using Harmonic Transfer Function (HTF) theory.

III. Harmonic Transfer Functions

A. Background

Transfer functions are an important tool in the analysis of LTI systems. An analogous tool for the analysis of LTP systems are Harmonic Transfer Functions (HTFs) [58]–[61].

The analysis of LTI systems is simplified by the fact that a sinusoidal input results in a sinusoidal output of the

same frequency. However, the frequency response of an LTP system not only includes the input frequency, but also the input frequency plus multiples of the fundamental ("pumping") frequency of the LTP system. Using the principle of harmonic balance, Wereley and Hall [58] showed that input–output relationship of a LTP system are determined by a possibly infinite parallel series of frequency shifted LTI subsystems. The transfer functions of these LTI sub-systems are called the HTFs of the LTP system.

B. State Space Representation of HTF

A generic LTP system can be defined as,

$$\begin{aligned} \dot{x}(t) &= A(t)x(t) + B(t)u(t), \\ y(t) &= C(t)x(t) + D(t)u(t). \end{aligned} \tag{5}$$

For such a system, Wereley and Hall [58] derived the Harmonic transfer functions using the state space representation and the principle of Harmonic Balance, which we review here. This representation is given by

$$\mathcal{H}(s) = \mathcal{C}\left[sI - (\mathcal{A} - \mathcal{N})^{-1}\right]\mathcal{B} + \mathcal{D}, \tag{6}$$

where $\mathcal{A}$, $\mathcal{B}$, $\mathcal{C}$,$\mathcal{D}$ are the doubly infinite Toeplitz matrices containing the Fourier coefficients of the system matrices $A(t)$, $B(t)$, $C(t)$, $D(t)$ respectively. Wereley and Hall [58] also showed that the elements $H_{n,m}(s)$ of $\mathcal{H}$, and the transfer functions of the LTI subsystems are related via $H_{n,m}(s) = H_{n-m}(s + jm\omega)$.

C. HTF's for Our Active Sensing System

Equation (6), for the simplifying case of time-constant A, B and time-varying C, reduces to the case of "LTI plant with modulated output" as described in [58], and has the following form:

$$\mathcal{H}_{n,m}(s) = C_{n-m}\left(s_m I - A\right)^{-1} B, \tag{7}$$

where $\mathcal{H}_{n,m}(s)$ are the elements of the doubly infinite $\mathcal{H}(s)$ and C_k's are the Fourier coefficients of $C(t)$.

To find an analytical expressions for the harmonics, we assume a simplified form for the sensory "scene," $s(\cdot)$, being observed by the system:

$$\begin{aligned} s(x_1) &= \frac{1}{2}d_1 x_1^2 + e_1 x_1, \\ \implies g(x_1) &= s'(x_1) = d_1 x_1 + e_1, \end{aligned} \tag{8}$$

where, d_1 and e_1 are arbitrary real coefficients.

Now for the system (4), the Fourier coefficients of C_k's of $C(t)$ are given by

$$C_0 = \begin{bmatrix} 0 & e_1 \end{bmatrix} \quad C_{\pm 1} = \begin{bmatrix} \pm a\omega\frac{jd_1}{2} & \frac{ad_1}{2} \end{bmatrix}$$

This gives the following form for H_0, H_1, and H_{-1}:

$$H_0(s) = \frac{e_1}{b + Ms} \quad H_{\pm 1}(s) = \frac{ad_1(s \pm j\omega)}{2s(b + Ms)} \tag{9}$$

The output of the LTP system (4) can now be represented as

$$\delta y = h_0 * u + (h_1 * u)e^{j\omega t} + (h_{-1} * u)e^{-j\omega t}, \tag{10}$$

where h_0, h_1, h_{-1} are the time-domain representations of $H_0(s)$, $H_1(s)$, $H_{-1}(s)$ respectively.

Note that the sensory scene chosen in this work only contains the zeroth and first harmonics. If the sensory scene (8) were to contain higher harmonics, then (10) below would only be an approximation of the original system (4) that neglects the higher harmonics. Given our use of low-pass filtering (Section IV) this approximation would nevertheless prove useful for more general scenes.

Simplifying (10) using $e^{j\omega t} = \cos(\omega t) + j\sin(\omega t)$ and the fact that h_{-1} and h_1 are complex conjugates gives the following:

$$\begin{aligned} \delta y &= h_0 * u + (h_1 * u)e^{j\omega t} + \left[(h_1 * u)e^{j\omega t}\right]^* \\ &= h_0 * u + 2\mathrm{Re}\left[(h_1 * u)e^{j\omega t}\right], \end{aligned} \tag{11}$$

and thus

$$\delta y = h_0 * u + 2\left[\mathrm{Re}(h_1) * u\right]\cos(\omega t) - 2\left[\mathrm{Im}(h_1) * u\right]\sin(\omega t). \tag{12}$$

Note that, from Equation (9), we have

$$\mathrm{Im}(H_1) = \frac{\alpha}{ms^2 + bs}, \tag{13}$$

where $\alpha = a(d_1/2)\omega$, has no pole-zero cancellations, while both H_0 and the real part of H_1 have a pole-zero cancellation, a fact used in Section IV.

IV. Framework for Extracting $\mathrm{Im}(H_1)$

After deriving the HTFs for the active sensing system under consideration in Section III, we noted that the imaginary part of first harmonic has no pole-zero cancellations (resulting in an observable system). So, if we were able to successfully extract it, we would be able to use it as the output of an equivalent system which is observable. Indeed, this is the crux of this paper. This section completes our framework of modulation (described above), demodulation, and low-pass filtering to extract the imaginary part of first harmonic which furnishes a new (observable) LTI system which is approximately equivalent to the original nonlinear system. See Fig. 1.

A. Extracting the Observable Harmonic

As can be seen from the output Equation (12), the first harmonic's imaginary part is modulated by a sinusoidal signal. So we demodulate (12) with a sinusoidal signal, which results in the following equation:

$$\begin{aligned} \delta y_{\mathrm{mod}} &= \delta y \sin\omega t \\ &= (h_0 * u)\sin\omega t + (\mathrm{Re}(h_1) * u)\sin 2\omega t \\ &\quad + (\cos 2\omega t - 1)\mathrm{Im}(h_1) * u \\ &= -\mathrm{Im}(h_1) * u + (h_0 * u)\sin\omega t \\ &\quad + (\mathrm{Re}(h_1) * u)\sin 2\omega t + (\mathrm{Im}(h_1) * u)\cos 2\omega t. \end{aligned} \tag{14}$$

After demodulation, the output is contaminated by the remaining harmonics (modulated by sinusoids at ω and 2ω). If we assume that $h_0 * u$, $\mathrm{Re}(h_1) * u$, and $\mathrm{Im}(h_1) * u$ are sufficiently band-limited signals, then it is possible, in

principle, to low-pass filter δy_{mod}, thereby extracting the first term $\text{Im}(h_1) * u$, which is at the base band (unmodulated). So, we pass the output from (14) through a low-pass filter, and assume that the modulated signals are eliminated:

$$\begin{aligned} \delta y_{\text{fil}} &= \delta y_{\text{mod}} * h_{\text{lpf}} \\ &= -h_{\text{lpf}} * \text{Im}(h_1) * u, \end{aligned} \tag{15}$$

where h_{lpf} represents the low-pass filter. Our system can now be seen as the cascade of the "Simplified System", $\text{Im}(H_1)$, and a low pass filter, as shown in Fig. 1b.

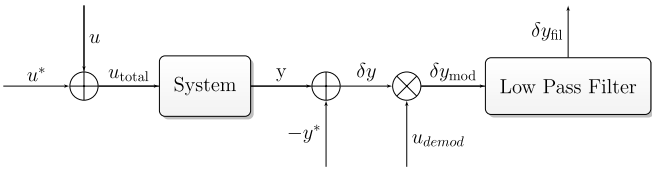

(a) Complete nonlinear system.

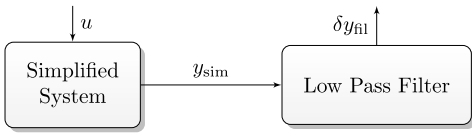

(b) Approximately equivalent system.

Fig. 1: Block diagrams.

B. Simulation

In order to compare the LTI system approximation and the complete (nonlinear) active sensing system, we simulate in MATLAB both the systems using an LQG controller.

1) System and Filter Parameters: The sensory scene is given by $s(x) = \frac{1}{2}d_1x^2 + e_1x$, introducing two parameters. Furthermore, the LTP plant model (4) in Section II has three parameters (m, b, and ω). The system ratio $\frac{b}{m}$ has been chosen based on the ratios of a weakly electric fish system [54], which has inspired this work. A 5^{th}-order Butterworth filter [62] with 0.5 Hz as a cut-off frequency has been used as the low-pass filter in (15).

2) State Estimation and Control: Since our equivalent LTI system is observable (no pole-zero cancellations), we can use the output for a state estimator. We implemented a Kalman filter (KF) [63] for this purpose. The initial covariance matrices for the KF are given in Table I. The estimated state is now fed through an infinite-horizon linear quadratic regulator (LQR) controller to try to control the system to a fixed goal position. The parameters used in our simulations are given in Table I.

C. Results

1) System Identification of Nonlinear System: To show that the developed LTI system and the nonlinear active sensing system are approximately equivalent, we compare the Bode plots of both systems in Fig. 2. Although these plots match each other at most frequencies, we note that at 1 Hz (which is half the "pumping" frequency) there is a mismatch between the Bode plots of the approximate LTI system and the nonlinear system. This is likely due to harmonic interactions between the control signal and the system's own harmonics. At higher frequencies, the Bode plots do not match due to interactions of higher harmonics and the control signal leaking through the low-pass filter.

Parameter	Description	Value	Units
m	System mass	1	kg
b	System damping	1.7	$\text{N}\cdot\text{s}\cdot\text{m}^{-1}$
ω	Pumping frequency	4π	$\text{rad}\cdot\text{s}^{-1}$
d_1	scene coefficient	3	m^{-2}
e_1	scene coefficient	5	m^{-1}
	Process Covariance (KF)	$10^{-4}I_{2\times2}$	
	Measurement Noise (KF)	0	
	State weights (LQR)	$2I_{2\times2}$	
	control weight (LQR)	1	

TABLE I: System and sensory scene parameters.

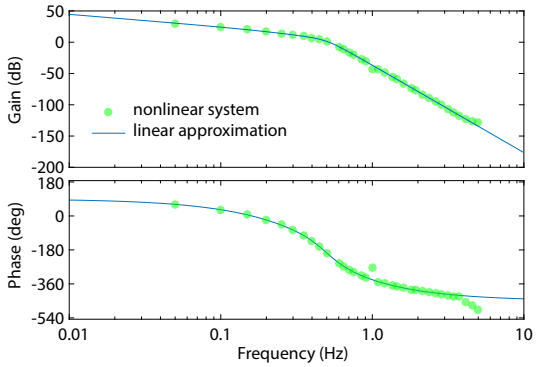

Fig. 2: The Bode plot of the complete (nonlinear) system agrees closely with that of the approximately equivalent linear system. Parameters in Table I.

2) LQG Control: To further validate our framework, we simulated the LQG system in Section IV-B. Fig. 3(a) demonstrates that the Kalman state estimate of position, $\widehat{\delta x_1}(t)$, of the approximately equivalent LTI system closely matches the relative position of the nonlinear active sensing system about the "active" movements of the system, i.e. $\delta x_1(t) = x_1(t) - x_1^*(t)$. The velocity state estimate also matches well (Fig. 3(b)). We also compare the output signal from the equivalent LTI system and to the δy_{fil} from the simulation of the nonlinear active sensing system in Fig. 3(c). Fig. 3(d) plots the position of the system along with it's active movements. This figure also shows how the sensory scene being observed by the system varies with time.

V. Conclusion

We developed a framework to recover observability via active sensing using HTF theory. Our central idea is that the higher harmonics of an active sensing system render the system observable. To illustrate this, we developed a biologically inspired active sensing system, where the output is a high-pass-filtered point measurement of the sensory scene. Controlling this system to a fixed point is shown to render it nonlinearly unobservable. The proposed active sensing framework involves modulation, demodulation, and

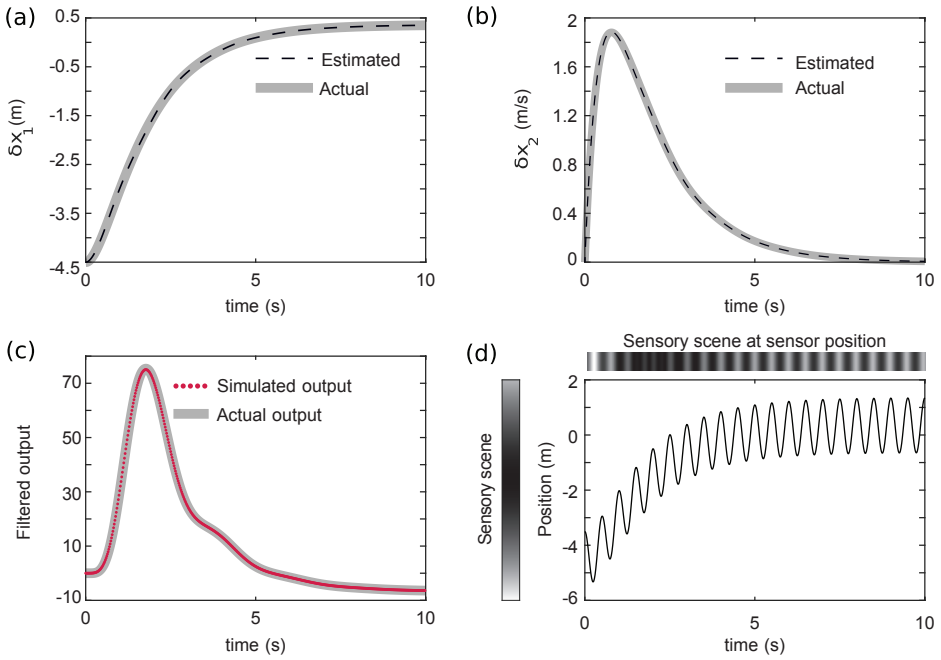

Fig. 3: Simulation and comparison of system states and outputs to validate the developed framework. Note that for this regime, the linear simulations closely matches the nonlinear system. The example shown in panels (a-c) start from an initial position, $\delta x_1 = -4.5$ to $\delta x_1 = 0.36$ relative to the equilibrium $(x_1^*, x_2^*) = (\cos \omega t, -\omega \sin \omega t)$, using the Kalman position estimate from the approximately equivalent observable system. (a) Comparison of position of linear and nonlinear system. (b) Comparison of velocity of linear and nonlinear system. (c) Comparison between the demodulated, filtered output signal from the nonlinear system and that of the simulated linear approximation. (d) Position of the nonlinear system. The gray map along the y-axis depicts the intensity of the sensory scene at an instant and the gray-map above the graph shows the scene intensity observed by the sensor at each time instant; recall that the sensor then high-pass filters this intensity measurement as the sensor output.

low-pass filtering the original system. This process recovers observability by transforming the system into an approximately equivalent, observable, LTI system.

To illustrate this framework, we tested it on the "simplest" biologically inspired system that requires active sensing. This system was chosen as it is easy to model, and thus enabled us to analytically calculate the HTF's of the system.

Future work can delve deeper into designing richer sensor models than the simple differentiator model used in this work. Also, the choices of the active motions and demodulating signals used to isolate the observable harmonic can be chosen to optimize some meaningful metric of the system such as an observability metric.

ACKNOWLEDGMENT

Thanks to Eric Fortune, Mert Ankarali, Andrew Lamperski and İsmail Uyanık for valuable comments and feedback. This material is based upon work supported by the National Science Foundation under Grant No. 1557858.

REFERENCES

[1] R. Bajcsy, "Active perception," *Proc IEEE*, vol. 76, no. 8, pp. 966–1005, 1988.

[2] M. E. Nelson and M. A. MacIver, "Sensory acquisition in active sensing systems," *J Comp Physiol A*, vol. 192, no. 6, pp. 573–586, 2006.

[3] S. A. Stamper, E. Roth, N. J. Cowan, and E. S. Fortune, "Active sensing via movement shapes spatiotemporal patterns of sensory feedback," *J Exp Biol*, vol. 215, no. 9, pp. 1567–1574, 2012.

[4] R. Ditchburn and B. Ginsborg, "Vision with a stabilized retinal image," *Nature*, vol. 170, no. 4314, pp. 36–37, 1952.

[5] C. F. Moss and A. Surlykke, "Auditory scene analysis by echolocation in bats," *J Acoust Soc Am*, vol. 110, no. 4, pp. 2207–2226, 2001.

[6] N. Ulanovsky and C. F. Moss, "What the bat's voice tells the bat's brain," *Proc Nat Acad Sci*, vol. 105, no. 25, pp. 8491–8498, 2008.

[7] T. H. Bullock, "Electroreception," *Annu Rev Neurosci*, vol. 5, no. 1, pp. 121–170, 1982.

[8] E. Ahissar and A. Arieli, "Figuring space by time," *Neuron*, vol. 32, no. 2, pp. 185–201, 2001.

[9] L. J. Fleishman and A. C. Pallus, "Motion perception and visual signal design in anolis lizards," *Proc Nat Acad Sci*, vol. 277, no. 1700, pp. 3547–3554, 2010.

[10] K. Ghose and C. F. Moss, "Steering by hearing: a bats acoustic gaze is linked to its flight motor output by a delayed, adaptive linear law," *J Neurosci*, vol. 26, no. 6, pp. 1704–1710, 2006.

[11] P. König and H. Luksch, "Active sensing-closing multiple loops," *Zeitschrift für Naturforschung C*, vol. 53, no. 7-8, pp. 542–549, 1998.

[12] S. J. Lederman and R. L. Klatzky, "Hand movements: A window into haptic object recognition," *Cog Psych*, vol. 19, no. 3, pp. 342–368, 1987.

[13] P. Madsen, I. Kerr, and R. Payne, "Echolocation clicks of two free-ranging, oceanic delphinids with different food preferences: false killer whales *Pseudorca crassidens* and Risso's dolphins *Grampus griseus*," *J Exp Biol*, vol. 207, no. 11, pp. 1811–1823, 2004.

[14] J. Najemnik and W. S. Geisler, "Optimal eye movement strategies in visual search," *Nature*, vol. 434, no. 7031, pp. 387–391, 2005.

[15] R. Peters, W. Loos, F. Bretschneider, and A. Baretta, "Electroreception in catfish: patterns from motion," *Belg J Zool*, no. 1, 1999.

[16] K. Sathian, "Tactile sensing of surface features," *Trends Neurosci*, vol. 12, no. 12, pp. 513–519, 1989.

[17] C. E. Schroeder, D. A. Wilson, T. Radman, H. Scharfman, and P. Lakatos, "Dynamics of active sensing and perceptual selection," *Curr Opin Neurobiol*, vol. 20, no. 2, pp. 172–176, 2010.

[18] C. Assad, B. Rasnow, and P. K. Stoddard, "Electric organ discharges and electric images during electrolocation," *J Exp Biol*, vol. 202, no. 10, pp. 1185–1193, 1999.

[19] D. Babineau, J. E. Lewis, and A. Longtin, "Spatial acuity and prey detection in weakly electric fish," *PLoS Comp Biol*, vol. 3, no. 3, p. e38, 2007.

[20] W. Heiligenberg, "Theoretical and experimental approaches to spatial aspects of electrolocation," *J Comp Physiol*, vol. 103, no. 3, pp. 247–272, 1975.

[21] M. A. MacIver, N. A. Patankar, and A. A. Shirgaonkar, "Energy-information trade-offs between movement and sensing," *PLoS Comp Biol*, vol. 6, no. 5, p. e1000769, 2010.

[22] E. Ahissar and A. Arieli, "Seeing via miniature eye movements: a dynamic hypothesis for vision," *Frontiers Comp Neurosci*, vol. 6, p. 89, 2012.

[23] D. H. Ballard, "Animate vision," *Artif Intell*, vol. 48, no. 1, pp. 57–86, 1991.

[24] A. Blake and A. Yuille, Eds., *Active Vision*. Cambridge, MA, USA: MIT Press, 1993.

[25] M. Brecht, B. Preilowski, and M. M. Merzenich, "Functional architecture of the mystacial vibrissae," *Behav Brain Res*, vol. 84, no. 1, pp. 81–97, 1997.

[26] G. E. Carvell and D. Simons, "Biometric analyses of vibrissal tactile discrimination in the rat," *J Neurosci*, vol. 10, no. 8, pp. 2638–2648, 1990.

[27] R. A. Grant, B. Mitchinson, C. W. Fox, and T. J. Prescott, "Active touch sensing in the rat: anticipatory and regulatory control of whisker movements during surface exploration," *J Neurophysiol*, vol. 101, no. 2, pp. 862–874, 2009.

[28] J. W. Gustafson and S. L. Felbain-Keramidas, "Behavioral and neural approaches to the function of the mystacial vibrissae." *Psychol Bull*, vol. 84, no. 3, p. 477, 1977.

[29] M. J. Hartmann, "Active sensing capabilities of the rat whisker system," *Auton Robot*, vol. 11, no. 3, pp. 249–254, 2001.

[30] V. Dürr, Y. König, and R. Kittmann, "The antennal motor system of the stick insect carausius morosus: anatomy and antennal movement pattern during walking," *J Comp Physiol A*, vol. 187, no. 2, pp. 131–144, 2001.

[31] B. Horseman, M. Gebhardt, and H. Honegger, "Involvement of the suboesophageal and thoracic ganglia in the control of antennal movements in crickets," *J Comp Physiol A*, vol. 181, no. 3, pp. 195–204, 1997.

[32] T. J. Prescott, M. E. Diamond, and A. M. Wing, "Active touch sensing," *Philos Trans R Soc B*, vol. 366, no. 1581, pp. 2989–2995, 2011.

[33] A. Saig, G. Gordon, E. Assa, A. Arieli, and E. Ahissar, "Motor-sensory confluence in tactile perception," *J Neurosci*, vol. 32, no. 40, pp. 14 022–14 032, 2012.

[34] S. Ranade, B. Hangya, and A. Kepecs, "Multiple modes of phase locking between sniffing and whisking during active exploration," *J Neurosci*, vol. 33, no. 19, pp. 8250–8256, 2013.

[35] M. Wachowiak, "All in a sniff: olfaction as a model for active sensing," *Neuron*, vol. 71, no. 6, pp. 962–973, 2011.

[36] D. W. Wesson, T. N. Donahou, M. O. Johnson, and M. Wachowiak, "Sniffing behavior of mice during performance in odor-guided tasks," *Chem Senses*, vol. 33, no. 7, pp. 581–596, 2008.

[37] E. S. Hassan, "Hydrodynamic imaging of the surroundings by the lateral line of the blind cave fish *Anoptichthys jordani*," in *The Mechanosensory Lateral Line*. Springer, 1989, pp. 217–227.

[38] J. C. Montgomery, S. Coombs, and C. F. Baker, "The mechanosensory lateral line system of the hypogean form of astyanax fasciatus," in *The biology of hypogean fishes*. Springer, 2001, pp. 87–96.

[39] C. Von Campenhausen, I. Riess, and R. Weissert, "Detection of stationary objects by the blind cave fish *Anoptichthys jordani* (*Characidae*)," *J Comp Physiol*, vol. 143, no. 3, pp. 369–374, 1981.

[40] J. Aloimonos, I. Weiss, and A. Bandyopadhyay, "Active vision," *Int J Comp Vis*, vol. 1, no. 4, pp. 333–356, 1988.

[41] P. Gao, B. Ploog, and H. Zeigler, "Whisking as a "voluntary" response: operant control of whisking parameters and effects of whisker denervation," *Somatosens Mot Res*, vol. 20, no. 3-4, pp. 179–189, 2003.

[42] J. J. Gibson, "Observations on active touch." *Psychol Rev*, vol. 69, no. 6, p. 477, 1962.

[43] C. B.-C. Hille, G. Dücker, and P. Guido Dehnhardt, "Haptic discrimination of size and texture in squirrel monkeys (*Saimiri sciureus*)," *Somatosens Mot Res*, vol. 18, no. 1, pp. 50–61, 2001.

[44] M. Lungarella, T. Pegors, D. Bulwinkle, and O. Sporns, "Methods for quantifying the informational structure of sensory and motor data," *Neuroinformatics*, vol. 3, no. 3, pp. 243–262, 2005.

[45] C. E. Raburn, K. J. Merritt, and J. C. Dean, "Preferred movement patterns during a simple bouncing task," *J Exp Biol*, vol. 214, no. 22, pp. 3768–3774, 2011.

[46] E. Visalberghi and C. Néel, "Tufted capuchins (*Cebus apella*) use weight and sound to choose between full and empty nuts," *Ecol Psychol*, vol. 15, no. 3, pp. 215–228, 2003.

[47] B. T. Hinson, M. K. Binder, and K. A. Morgansen, "Path planning to optimize observability in a planar uniform flow field," in *Proc Amer Control Conf*. IEEE, 2013, pp. 1392–1399.

[48] S. Cedervall and X. Hu, "Nonlinear observers for unicycle robots with range sensors," *IEEE Trans Autom Control*, vol. 52, no. 7, p. 1325, 2007.

[49] P. Salaris, R. Spica, P. R. Giordano, and P. Rives, "Online optimal active sensing control," in *Proc IEEE Int Conf Robot Autom*. IEEE, 2017, pp. 672–678.

[50] G. L. Mariottini, S. Martini, and M. B. Egerstedt, "A switching active sensing strategy to maintain observability for vision-based formation control," in *Proc IEEE Int Conf Robot Autom*. IEEE, 2009, pp. 2637–2642.

[51] E. Lalish, K. A. Morgansen, and T. Tsukamaki, "Oscillatory control for constant-speed unicycle-type vehicles," in *Proc IEEE Int Conf on Decision Control*. IEEE, 2007, pp. 5246–5251.

[52] B. T. Hinson and K. A. Morgansen, "Observability optimization for the nonholonomic integrator," in *Proc Amer Control Conf*. IEEE, 2013, pp. 4257–4262.

[53] N. J. Cowan and E. S. Fortune, "The critical role of locomotion mechanics in decoding sensory systems," *J Neurosci*, vol. 27, no. 5, pp. 1123–1128, 2007.

[54] S. Sefati, I. D. Neveln, E. Roth, T. R. Mitchell, J. B. Snyder, M. A. MacIver, E. S. Fortune, and N. J. Cowan, "Mutually opposing forces during locomotion can eliminate the tradeoff between maneuverability and stability," *Proc Nat Acad Sci*, vol. 110, no. 47, pp. 18 798–18 803, 2013.

[55] N. J. Cowan, M. M. Ankarali, J. P. Dyhr, M. S. Madhav, E. Roth, S. Sefati, S. Sponberg, S. A. Stamper, E. S. Fortune, and T. L. Daniel, "Feedback control as a framework for understanding tradeoffs in biology," *Integr Comp Biol*, vol. 54, no. 2, pp. 223–237, 2014.

[56] E. Roth, K. Zhuang, S. A. Stamper, E. S. Fortune, and N. J. Cowan, "Stimulus predictability mediates a switch in locomotor smooth pursuit performance for *Eigenmannia virescens*." *J Exp Biol*, vol. 214, no. 7, pp. 1170–1180, 2011.

[57] H. Nijmeijer and A. Van der Schaft, *Nonlinear dynamical control systems*. Springer Science & Business Media, 2013.

[58] N. M. Wereley, "Analysis and control of linear periodically time varying systems," Ph.D. dissertation, Massachusetts Institute of Technology, 1990.

[59] M. M. Ankarali and N. J. Cowan, "System identification of rhythmic hybrid dynamical systems via discrete time harmonic transfer functions," in *Proc IEEE Int Conf on Decision Control*. IEEE, 2014, pp. 1017–1022.

[60] A. Siddiqi, "Identification of the harmonic transfer functions of a helicopter rotor," Ph.D. dissertation, Massachusetts Institute of Technology, 2001.

[61] N. M. Wereley and S. R. Hall, "Frequency response of linear time periodic systems," in *Proc IEEE Int Conf on Decision Control*. IEEE, 1990, pp. 3650–3655.

[62] S. Butterworth, "On the theory of filter amplifiers," *Wireless Engineer*, vol. 7, no. 6, pp. 536–541, 1930.

[63] R. E. Kalman, "A new approach to linear filtering and prediction problems," *Trans ASME*, vol. 82, no. Series D, pp. 35–45, 1960.